

10- μm InGaAsP/InP SPADs for 1064 nm detection with 36% PDP and 118 ps timing jitter

Utku Karaca¹, Ekin Kizilkan¹, Claudio Bruschini¹, and Edoardo Charbon¹

¹École Polytechnique Fédérale de Lausanne (EPFL), Neuchâtel, Switzerland

emails: utku.karaca@epfl.ch, ekin.kizilkan@epfl.ch, claudio.bruschini@epfl.ch, and edoardo.charbon@epfl.ch

Abstract—In this work, we present a family of planar InGaAsP/InP SPADs with a diameter of 10 μm targeting 1064 nm wavelength detection. TCAD simulations enabled the determination of Zn diffusion depths, thereby achieving low noise and uniform photoresponse. Devices with 1.5- μm , 1.3- μm , and 0.75- μm multiplication region thicknesses were fabricated. The device with a 1.5- μm multiplication region demonstrated 53 kcps DCR, 118 ps timing jitter at 5 V_{ex} , and 36% PDP at 9 V_{ex} . The measurements were done from the backside without a metal reflector, all at 300K. The DCR was reduced to 14.1 kcps at 273K, 5.5 kcps at 253K, and 2.75 kcps at 225K at 5 V_{ex} . The operating frequency can be increased up to 500 kHz with only 11.8% and to 200 kHz with 5.8% afterpulsing at 300K. The active area scanning results indicated that the photoresponse is almost flat at and above 5 V_{ex} . Thinner multiplication regions showed higher PDPs and lower jitter, at a cost of higher noise.

I. INTRODUCTION

Single-photon detection at 1064 nm wavelength is useful in long-haul light detection and ranging (LiDAR) and in free-space communications [1]. Medical applications, such as time-gated diffuse correlation spectroscopy for blood flow measurements can also make use of such a detector [2]. High-power 1064 nm Nd:YAG lasers enable a variety of similar experiments and are appealing to diversify the applications. Since the photon detection probability (PDP) of CMOS-based SPADs reduces towards near-infrared (NIR) due to the low silicon absorption coefficient, superconducting nanowire single-photon detectors (SNSPDs) and InGaAsP/InP single-photon avalanche diodes (SPADs) have emerged as the best alternatives to develop single-photon cameras operating at 1064 nm. However, InGaAsP/InP SPADs perform well at much higher temperatures than SNSPDs, and even at room temperature, enabling scalable and compact solutions that are cost-effective as well.

II. RESULTS

SPADs utilize a separate absorption-charge-multiplication (SACM) structure and the double zinc (Zn) diffusion technique to form the multiplication and guard ring (GR) regions (Fig. 1). The n-contact was carried to the top surface, allowing to illuminate SPADs from the backside. The absorber thickness is 1 μm , and the charge layer doping is larger than $2 \times 10^{17} \text{ cm}^{-3}$ to keep the electric field sufficient to deplete the absorber before breakdown is reached (Fig. 2). We designed, fabricated, and fully characterized 10- μm diameter SPADs with 1.5- μm , 1.3- μm , and 0.75- μm multiplication region thickness.

According to avalanche breakdown probability simulations in TCAD, a 0.5- μm depth difference between shallow and deep Zn diffusions was the preferred solution. This could potentially provide lower noise at the cost of a less uniform photoresponse over the active area (Fig. 3). The SEM image of the fabricated device with a 1.3- μm multiplication region prove that the Zn diffusion depths are close to the planned values (Fig. 4). The measured I-V curves at 300K indicate the avalanche breakdown and punch-through voltages for each device (Fig. 5). In the remaining measurements, the SPADs were operated in time-gating mode with 50 k Ω ballast resistor and a 100 ns gate-on time. The gating frequency sweep of each device showed that devices can be operated up to 500 kHz with low afterpulsing probability (APP) at 300K (Fig. 6). With 10 kHz gating, a median DCR of 53 kcps was obtained with a multiplication region thickness of 1.5- μm , 302 kcps with 1.3 μm , and 2130 kcps with 0.75 μm , where the DCR was normalized with gate-on time. The median DCR was reduced to 14.1 kcps at 273K, 5.5 kcps at 253K, and 2.75 kcps at 225K, for a 1.5- μm multiplication region at 5 V_{ex} (Fig. 7). Active area scanning was performed with a 1060 nm pulsed laser, demonstrating that the response difference between the edge and center of the active region becomes smaller when increasing V_{ex} , and that a uniform response can be achieved at and above 5 V_{ex} (Fig. 8). The PDP obtained with a monochromator and wide-spectrum lamp at 1060 nm and 5 V_{ex} was 19.5% for 1.5- μm multiplication region thickness, 20.4% for 1.3 μm , and 21.5% for 0.75 μm (Fig. 9). A high PDP of 36% at 9 V_{ex} was achieved with a 1.5- μm multiplication. Inter-arrival avalanche histograms indicated that APPs of only 11.1% and 5.8% can be achieved at 500 kHz and 200 kHz gating and 300K, respectively (Fig. 10). The timing jitter was acquired via time-correlated single-photon counting (TCSPC), yielding as 118.4 ps, 110 ps, and 84 ps (FWHM) after deconvolution (Fig. 11). The comparison with state-of-the-art InGaAsP SPADs shows that fabricated devices achieved the smallest sizes, with high PDP, and low timing jitter (Fig. 12), while further optimization is to be expected.

REFERENCES

- [1] L. Xue, Z. Li, L. Zhang, D. Zhai, Y. Li, S. Zhang, M. Li, L. Kang, J. Chen, P. Wu *et al.*, “Satellite laser ranging using superconducting nanowire single-photon detectors at 1064 nm wavelength,” *Optics letters*, vol. 41, no. 16, pp. 3848–3851, 2016.
- [2] C.-S. Poon, D. S. Langri, B. Rinehart, T. M. Rambo, A. J. Miller, B. Foreman, and U. Sunar, “First-in-clinical application of a time-gated diffuse correlation spectroscopy system at 1064 nm using superconducting nanowire single photon detectors in a neuro intensive care unit,” *Biomedical Optics Express*, vol. 13, no. 3, pp. 1344–1356, 2022.

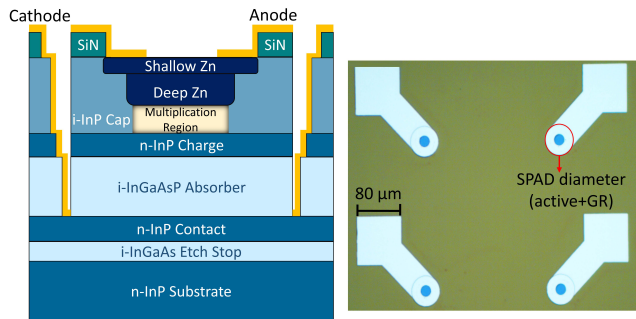


Fig. 1: The cross-section and an optical image of fabricated SPADs.

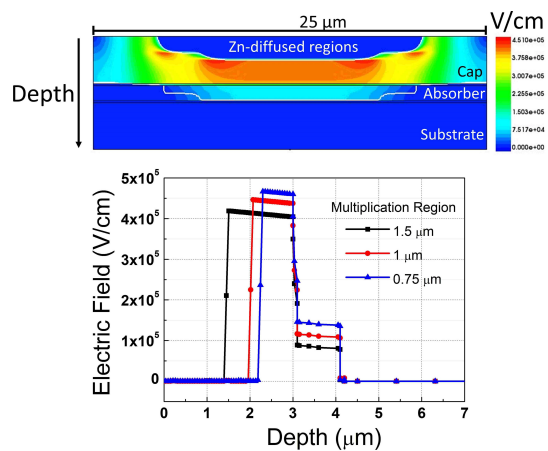


Fig. 2: Electric field simulations in TCAD at 300K.

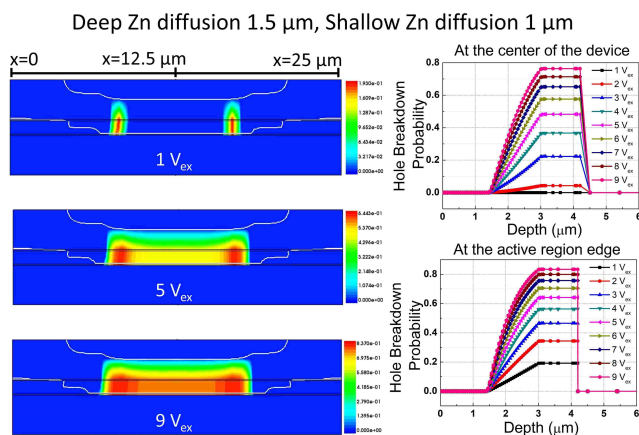


Fig. 3: Avalanche breakdown probability simulations for devices with a 0.5- μm Zn diffusion depth difference at 300K.

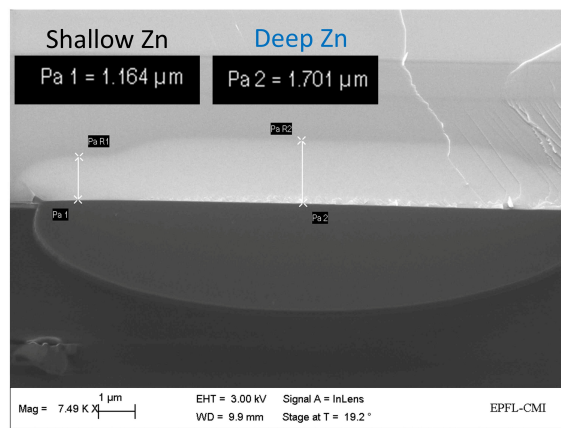


Fig. 4: SEM image belonging to a device with a 1.3- μm multiplication region.

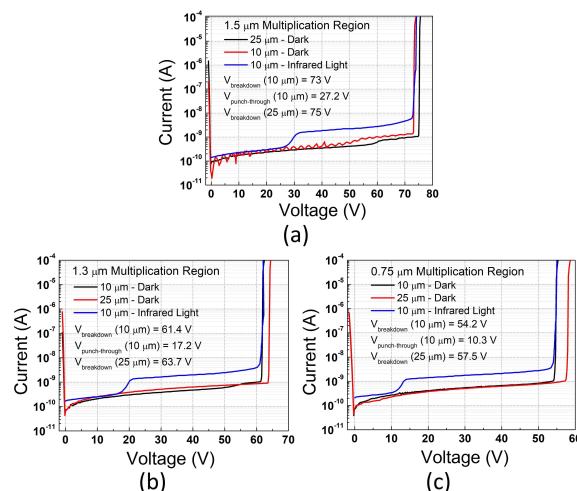


Fig. 5: I-V characteristics of the devices with (a) 1.5- μm , (b) 1.3- μm , and (c) 0.75- μm multiplication regions at 300K.

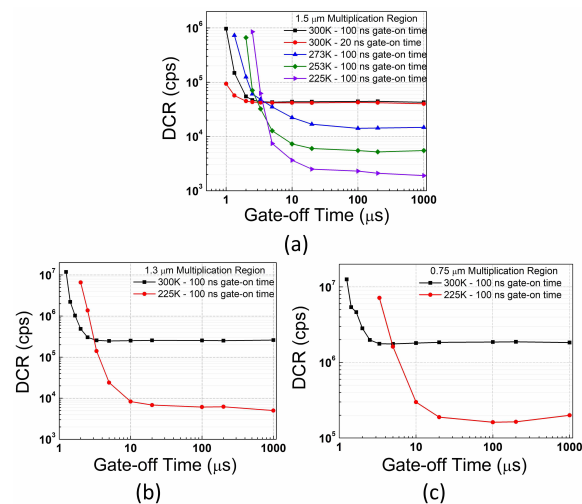


Fig. 6: Gating frequency sweep of the devices with (a) 1.5- μm , (b) 1.3- μm , and (c) 0.75- μm multiplication regions.

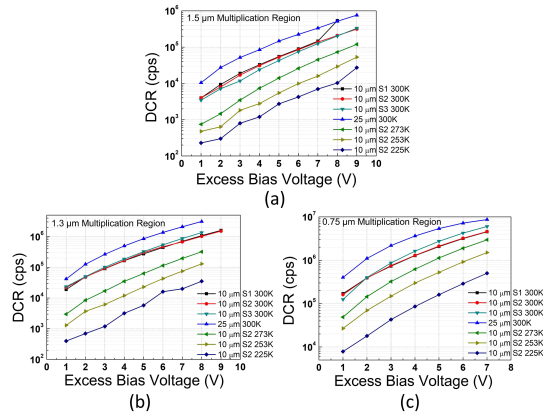


Fig. 7: DCR measurements of the devices with (a) 1.5- μm , (b) 1.3- μm , and (c) 0.75- μm multiplication regions with 10 kHz gating and 100 ns gate-on time. Note: Three devices (S1, S2, and S3) were characterized with a 10- μm diameter. S2 corresponds to the median device.

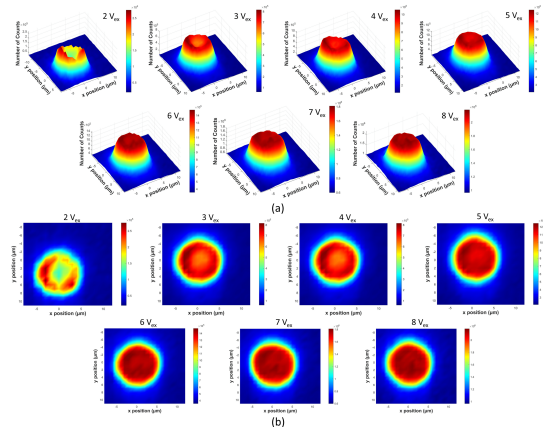


Fig. 8: Active area scanning of the SPAD with a 1.3- μm multiplication region from the (a) side and (b) top view by utilizing a 1060 nm pulsed laser at 300K.

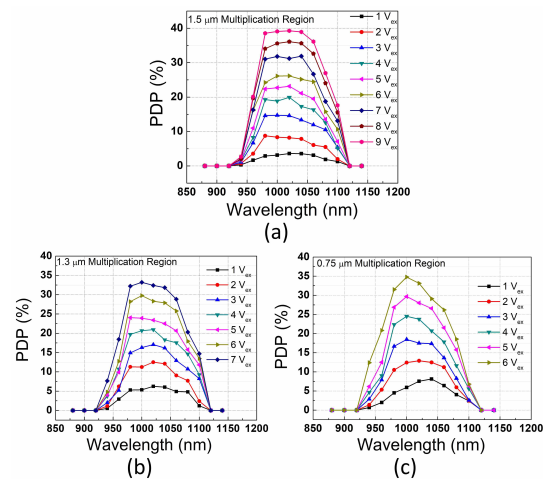


Fig. 9: PDP measurements of the devices with (a) 1.5- μm , (b) 1.3- μm , and (c) 0.75- μm multiplication regions at 300K and with 10 kHz gating and 100 ns gate-on time.

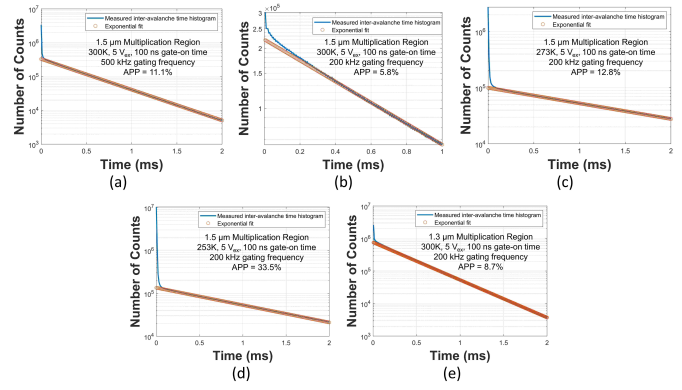


Fig. 10: Inter-arrival avalanche pulse histograms of the devices at various temperatures and gating frequencies with 100 ns gate-on time.

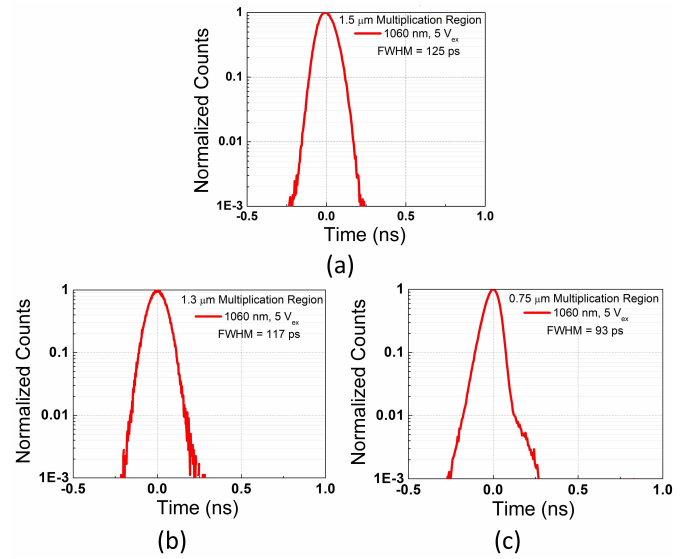


Fig. 11: Timing jitter measurements of the devices with (a) 1.5- μm , (b) 1.3- μm , and (c) 0.75- μm multiplication regions at 300K.

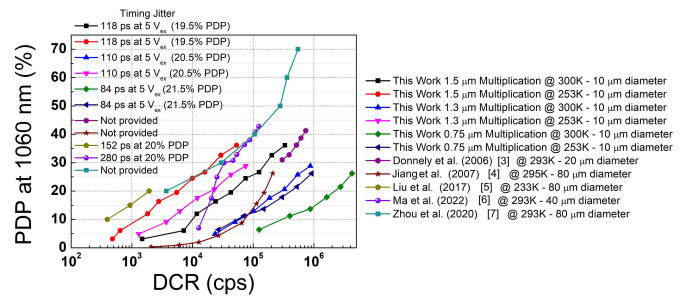


Fig. 12: Comparison of the developed SPADs with the state-of-the-art InGaAsP SPADs targeting 1064 nm detection.

[3] J. P. Donnelly, E. K. Duerr, K. A. McIntosh, E. A. Dauler, D. C. Oakley, S. H. Groves, C. J. Vineis, L. J. Mahoney, K. M. Molvar, P. I. Hopman et al., "Design considerations for 1.06- μm InGaAsP- InP geiger-mode avalanche photodiodes," *IEEE Journal of Quantum Electronics*, vol. 42, no. 8, pp. 797–809, 2006.
 [4] X. Jiang, M. A. Itzler, R. Ben-Michael, and K. Slomkowski, "InGaAsP- InP avalanche photodiodes for single-photon detection," *IEEE Journal of selected topics in quantum electronics*, vol. 13, no. 4, pp. 895–905, 2007.
 [5] J. Liu, T. Zhang, Y. Li, L. Ding, J. Tao, Y. Wang, Q. Wang, and J. Fang, "Design and characterization of free-running InGaAsP single-photon detector with active-quenching technique," *Journal of Applied Physics*, vol. 122, no. 1, 2017.
 [6] Y. Ma, Y. Gu, X. Li, B. Yang, X. Zhao, T. Li, Y. Zhang, H. Gong, and J. Fang, "InGaAsP/ InP geiger-mode avalanche photodiode towards sub-kHz dark count rate at 20% photon detection efficiency," *Journal of Lightwave Technology*, vol. 40, no. 22, pp. 7364–7374, 2022.
 [7] M. Zhou, W. Wang, H. Gu, H. Han, Y. Zhu, Z. Guo, L. Gui, X. Wang, and W. Lu, "InGaAsP/ InP single photon avalanche diodes with ultra-high photon detection efficiency," *Optical and Quantum Electronics*, vol. 52, pp. 1–9, 2020.